Piezoresistance Effect in p-Type PbTe†

J. RICHARD BURKE, JR.
U. S. Naval Ordnance Laboratory, Silver Spring, Maryland
and
The Catholic University of America, Washington, D. C.
(Received 17 March 1967)

We have measured the piezoresistance effect in 21 samples of p-type PbTe taken from single crystals grown by the Czochralski technique. The piezoresistance coefficients π_{11}, π_{12}, and π_{44} were obtained by application of hydrostatic pressure and of uniaxial stress in the [100], [111], and [110] crystallographic directions. The temperature dependence of these coefficients was investigated in the range 300 to 77°K for hole concentrations between 4.04×10^{17} and 4.97×10^{19} cm^{-3}. The temperature and carrier-concentration dependence of the shear coefficient π_{44} was clearly in qualitative agreement with a ⟨111⟩ multivalley model for the principal valence band, and the shear deformation potential Ξ_μ was found to be 8.5 eV. The experimental values of π_{44}, however, were much larger at all temperatures and carrier concentrations than those calculated using previously reported band parameters in existing theory. The theory was extended by means of a nonparabolic-band model, and calculations for degenerate statistics were made. This resulted in poorer agreement with experiment. Large values of the hydrostatic coefficient $\pi_{11}+2\pi_{12}$ were observed. They are attributed to the volume dependence of the transverse effective mass m_T of the ⟨111⟩ band and to the population of a second valence band. The deformation potential E_2 of the gap between the two valence bands was found to be −1.0 eV. Large values of the shear coefficient $\pi_{11}-\pi_{12}$ were also observed. However, the temperature dependence of this coefficient shows that this is not the result of the population of the nearby ⟨110⟩ valence band suggested by recent band calculations.

I. INTRODUCTION

LEAD TELLURIDE (PbTe) crystallizes in the face-centered cubic (fcc) lattice and has point-group symmetry $m3m$. Early work[1] on this material showed that it was a direct gap semiconductor with a small energy gap between the principal valence and conduction bands of 0.32 eV at 300°K. Optical[2] and magneto-optical[3] measurements have shown that this gap decreases significantly in going to lower temperatures. This is in contrast to most semiconductors which have a negative temperature coefficient of the gap. Despite this small gap, PbTe is an extrinsic material in which the carriers are generated by deviations from stoichiometry and which has the unusual feature, characteristic of the lead salts in general, that no freeze out of these carriers into "impurity" states is detectable for temperatures as low as 1.2°K. This result is consistent with "impurity" states which lie in the band because of the high-static dielectric constant of about 400. (See Refs. 4–8.)

Weak-field magnetoresistance,[9–11] piezoresistance,[12,13] measurements of the de Haas–van Alphen[14] and Shubnikov–de Haas[15,16] effects, and Azbel-Kaner cyclotron resonance[17–20] are each consistent with a ⟨111⟩ multivalley model in which the extrema of the principal conduction and valence bands are located at the L points of the Brillouin zone in which a constant-energy surface consists of four prolate elliposids of revolution for energies near the extrema. These constant-energy surfaces and the Brillouin zone for the fcc lattice are shown in Fig. 1. However, for some of the higher carrier concentrations in the range we have investigated, it has been shown[15,16,21] that the effective mass in the valence band is a function of energy and the constant-

† This paper is based on a thesis submitted to The Catholic University in partial fulfillment of the requirements for the Doctor of Philosophy degree in physics. Copies of the complete thesis are available from the Naval Ordnance Laboratory (see Ref. 35).

[1] W. W. Scanlon, in *Solid State Physics*, edited by F. Seitz and D. Turnbull (Academic Press Inc., New York, 1959), Vol. 9, p. 83.

[2] A. F. Gibson, Proc. Phys. Soc. (London) **B65**, 378 (1952).

[3] D. L. Mitchell, E. D. Palik, and J. N. Zemel, in *Proceedings of the International Conference on the Physics of Semiconductors, Paris, 1964* (Dunod Cie., Paris, 1964), p. 325.

[4] R. S. Allgaier and W. W. Scanlon, Phys. Rev. **111**, 1029 (1958).

[5] R. Kanai and K. Shohno, J. Appl. Phys. (Japan) **1**, 239 (1962).

[6] H. M. Day, Proc. IEEE **51**, 1362 (1963).

[7] N. Watanabe, J. Appl. Phys. (Japan) **3**, 166 (1964).

[8] W. Cochran, Phys. Letters **13**, 193 (1964).

[9] K. Shogenji and S. Uchiyama, J. Phys. Soc. Japan **12**, 1164 (1957).

[10] R. S. Allgaier, Phys. Rev. **119**, 554 (1960).

[11] R. S. Allgaier, in *Proceedings of the International Conference on the Physics of Semiconductors, Prague, 1960* (Czechoslovak Academy of Sciences, Prague, 1961), p. 1037.

[12] L. E. Hollander and T. J. Diesel, J. Appl. Phys. **31**, 692 (1960).

[13] J. R. Burke, B. B. Houston, and R. S. Allgaier, Bull. Am. Phys. Soc. **6**, 136 (1961).

[14] P. J. Stiles, E. Burstein, and D. N. Langenberg, J. Appl. Phys. **32**, 2174 (1961).

[15] K. F. Cuff, M. R. Ellett, and C. D. Kuglin, in *Proceedings of the International Conference on the Physics of Semiconductors, Exeter, 1962* (The Institute of Physics and The Physical Society, London, 1962), p. 316.

[16] K. F. Cuff, M. R. Ellett, C. D. Kuglin, and L. R. Williams, in *Proceedings of the International Conference on the Physics of Semiconductors, Paris, 1964* (Dunod Cie., Paris, 1964), p. 677.

[17] P. J. Stiles, E. Burstein, and D. N. Langenberg, in *Proceedings of the International Conference on the Physics of Semiconductors, Exeter, 1962* (The Institute of Physics and The Physical Society, London, 1962), p. 557.

[18] R. Nii, J. Phys. Soc. Japan **19**, 58 (1964).

[19] H. Numata and Y. Uemura, Phys. Letters **9**, 227 (1964).

[20] See Ref. 19, J. Phys. Soc. Japan **19**, 2140 (1964).

[21] J. R. Dixon and H. R. Riedl, Phys. Rev. **138**, A873 (1965).

energy surfaces deviate slightly from ellipsoids of revolution.

Evidence for the population of a second, lower-energy valence band has been found in the temperature[22,23] and pressure[24] dependence of the Hall coefficient and in the temperature dependence of the electric susceptibility mass.[21] Optical absorption data[25] suggest that the gap between the two valence bands is about 0.08 eV at 300°K ,while analysis of the temperature dependence of the Hall coefficient results in a gap of about 0.15 eV at 0°K.

Several scattering mechanisms have been proposed for the lead salts.[26–29] While some success has been achieved in explaining either the temperature and carrier concentration dependence or the magnitude of the observed mobility, it has not been possible to explain both.

In addition to the results of the first piezoresistance measurements on PbTe given in Refs. (12, 13), other studies, more limited in extent than the present investigation, have also been presented or published. These are summarized in Refs. 30–33. The purpose of this paper is to use the complete piezoresistance tensor to investigate the details of the band structure and transport properties over a wide range of temperature and carrier concentration.

II. THEORY

The piezoresistance coefficients are the components of a fourth-rank tensor which relates the components of one second-rank tensor, the applied stress, to the components of another second-rank tensor, the change in resistivity.[34,35] However, because both the stress and resistivity tensors are symmetric, it is convenient to express the relationship between them in matrix notation.[34] This relationship is exactly analogous to that between the stress and strain in elasticity theory.[36] For a cubic crystal with point-group symmetry $m3m$, there are only three independent piezoresistance coefficients π_{11}, π_{12}, and π_{44}. (See Ref. 37.)

An elastoconductance tensor is also defined. Its components relate the strain tensor to the change in conductivity.[34,35] In matrix notation, the independent components of the elastoconductance tensor are m_{11}, m_{12}, and m_{44}. They are simply related to π_{11}, π_{12}, and π_{44} by the elastic constants.[34,38] The elastoconductance coefficients are more convenient to deal with theoretically, but the piezoresistance coefficients are the quantities usually measured.

A. Large Shear Piezoresistance

As was first shown experimentally by Smith[38] and theroretically by Herring,[39] application of the appropriate shear stress will remove the degeneracy of some of the extrema in a multivalley model. The result is a transfer of electrons from the higher-energy to the lower-energy valleys. This is indicated schematically in Fig. 2. Although the average mobility of the carriers might be isotropic before the crystal was strained, if the mobility of the carriers in each valley is anisotropic, the average mobility after the strain will be anisotropic also. The result is a large change in resistivity in certain crystallographic directions. Since this change occurs only for the shear strain which removes the degeneracy, a study of the resistivity change as a function of the crystallographic orientation of the strain can be used

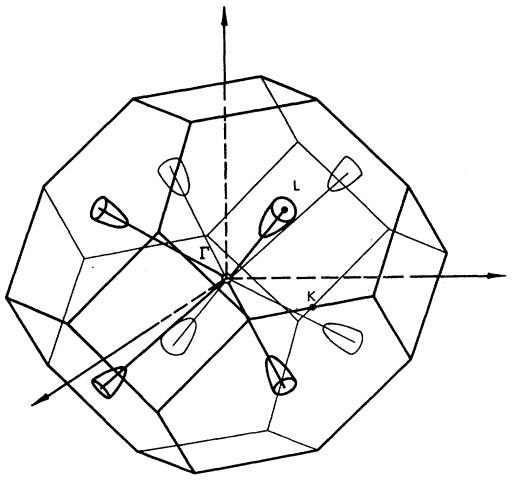

FIG. 1. Brillouin zone for the face-centered-cubic lattice and the ⟨111⟩ hole or electron ellipoids at the L points.

[22] R. S. Allgaier, J. Appl. Phys. **32**, 2185 (1961).
[23] R. S. Allgaier and B. B. Houston, Jr., J. Appl. Phys. **37**, 302 (1966).
[24] Y. Sato, M. Fujimoto, and A. Kobayashi, J. Phys. Soc. Japan **19**, 24 (1964).
[25] H. R. Riedl, Phys. Rev. **127**, 162 (1962).
[26] R. L. Petritz and W. W. Scanlon, Phys. Rev. **97**, 1620 (1955).
[27] M. N. Vinogradova, O. A. Golikova, B. A. Efimova, V. A. Kutasov, T. S. Stavitskaya, L. S. Stil'bans, and L. M. Sysoeva, Fiz. Tverd. Tela **1**, 1333 (1959) [English transl.: Soviet Phys.—Solid State **1**, 1224 (1960)].
[28] R. S. Allgaier and B. B. Houston, Jr., in *Proceedings of the International Conference on the Physics of Semiconductors, Exeter, 1962* (The Institute of Physics and The Physical Society, London, 1962), p. 172.
[29] B. S. Krishnamurthy and K. P. Sinha, J. Phys. Chem. Solids **26**, 1949 (1965).
[30] Yu. V. Ilisavskii, Fiz. Tverd. Tela **4**, 918 (1962) [English transl.: Soviet Phys.—Solid State **4**, 674 (1962)].
[31] J. R. Burke, Bull. Am. Phys. Soc. **8**, 310 (1963).
[32] R. Ito and K. Shogenji, J. Phys. Soc. Japan **18**, 1343 (1963).
[33] K. Shogenji and R. Ito, J. Phys. Soc. Japan **20**, 172 (1965).
[34] R. W. Keyes, in *Solid State Physics*, edited by F. Seitz and D. Turnbull (Academic Press Inc., New York, 1960), Vol. 11, p. 149.
[35] J. R. Burke, Naval Ordnance Laboratory Technical Report No. 66-55 (unpublished).
[36] J. F. Nye, *Physical Properties of Crystals* (Clarendon Press, London, 1960), p. 134.
[37] C. S. Smith, in *Solid State Physics*, edited by F. Seitz and D. Turnbull (Academic Press Inc., New York, 1958), Vol. 6, p. 237.
[38] C. S. Smith, Phys. Rev. **94**, 42 (1954).
[39] C. Herring, Bell System Tech. J. **34**, 237 (1955).

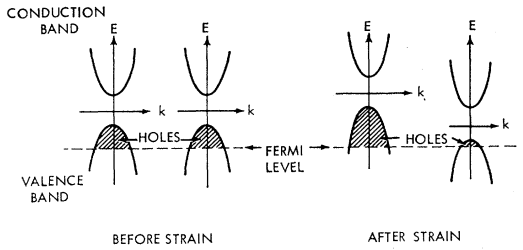

FIG. 2. Effect of a particular shear strain on two of the ⟨111⟩ valleys of the valence and conduction bands of PbTe.

to determine the existence of a multivalley model and the location of the extrema in the Brillouin zone.

Expressions for the large shear coefficient in various multivalley models have been derived for classical statistics by Herring,[39] Herring and Vogt,[40] Keyes,[34] and Pikus and Bir.[41] This theory was extended to include Fermi-Dirac statistics by Keyes[34] and Pollack,[42] and for a ⟨111⟩ multivalley model we have

$$\pi_{44}=\frac{\Xi_u}{3C_{44}kT}\frac{K-1}{2K+1}\frac{\mathfrak{F}_{s-1/2}(\eta)}{\mathfrak{F}_{s+1/2}(\eta)} \tag{1}$$

and

$$\pi_{11}=\pi_{12}=0,$$

when only the carrier transfer effect leads to a change in resistance. Ξ_u is one of the three independent deformation potential constants in a cubic crystal. As originally defined by Herring,[39] Ξ_u is the energy shift of the valley extremum produced by a tensile strain of magnitude u along the symmetry axis of the valley combined with a compressional strain of magnitude $u/2$ in the two directions perpendicular to each other and to the symmetry axis. For a ⟨111⟩ model, the symmetry axis of each valley lies in a ⟨111⟩ direction. $K=\mu_T/\mu_L$ is the ratio of the mobilities perpendicular and parallel to the symmetry axis, C_{44} is a shear elastic constant, k is Boltzmann's constant, T is the absolute temperature, and $\mathfrak{F}_j(\eta)$ is a Fermi-Dirac function of order j defined by

$$\mathfrak{F}_j(\eta)=\frac{1}{\Gamma(j+1)}\int_0^\infty\frac{\epsilon^j d\epsilon}{1+\exp(\epsilon-\eta)}, \tag{2}$$

where η is the Fermi level in units of kT relative to the band edge and Γ is the γ function. Since we will always be talking about conduction by holes, energies below the top of the valence band will be considered positive. The Fermi-Dirac functions defined by Eq. (2) have been tabulated by Blakemore.[43] They differ from the conventional Fermi-Dirac integrals[44] by the factor $1/\Gamma(j+1)$, but as explained by Dingle,[45] are mathematically more convenient. The ratio of Fermi-Dirac functions, which from this point on will be called the F-D factor, depends on the scattering index s defined by the relationship

$$\tau=\tau(0)E^s, \tag{3}$$

where τ is the relaxation time and E is the carrier energy relative to the band edge. For a carrier concentration p, the argument η is determined by

$$p=2(2\pi m_D kT/h^2)^{3/2}\mathfrak{F}_{1/2}(\eta) \tag{4}$$

for a parabolic band. Thus the F-D factor is an implicit function of the density of states mass m_D which is defined by

$$m_D=\nu^{2/3}(m_T m_T m_L)^{1/3}, \tag{5}$$

where ν is the number of valleys and m_T and m_L are, respectively, the transverse and longitudinal effective mass of each valley.

For classical statistics, the F-D factor goes to one and Eq. (1) becomes

$$\pi_{44}=\frac{\Xi_u}{3C_{44}kT}\frac{K-1}{2K+1}\quad\text{(classical statistics)}. \tag{6}$$

Since Ξ_u, C_{44}, and K are not usually strong functions of temperature, Eq. (6) predicts an inverse temperature dependence for π_{44} in this limit. Also, since K can be determined independently from weak-field magnetoresistance measurements, Eq. (6) can be used to determine the deformation potential constant Ξ_u.

For completely degenerate statistics, Eq. (1) becomes

$$\pi_{44}=\frac{\Xi_u}{3C_{44}kT}\frac{K-1}{2K+1}\frac{s+\frac{3}{2}}{E_F}\quad\text{(degenerate statistics)}. \tag{7}$$

In this limit π_{44} is temperature-independent.

B. Effects of Hydrostatic Pressure

Each of the coefficients π_{11} and π_{12} describes the effect on the resistance of a combination of pure shear stress and hydrostatic pressure. The effect of hydrostatic pressure only is given by the coefficient

$$\pi_H=\pi_{11}+2\pi_{12} \tag{8}$$

for a cubic crystal with point-group symmetry $m3m$.

1. Two-Band Conduction

A large contribution to π_H in an *extrinsic* semiconductor may occur when conductivity takes place in two or more bands having carriers of the same sign because of the change in energy gap between them. When two valence bands conduct,

$$\sigma=p_1e\mu_1+p_2e\mu_2, \tag{9}$$

[40] C. Herring and E. Vogt, Phys. Rev. **101**, 944 (1955).
[41] G. E. Pikus and G. L. Bir, Fiz. Tverd. Tela **4**, 2090 (1962) [English transl.: Soviet Phys.—Solid State **4**, 1530 (1963)].
[42] M. Pollack, Phys. Rev. **111**, 798 (1958).
[43] J. S. Blakemore, *Semiconductor Statistics* (Pergamon Press, Inc., New York, 1962), p. 346.
[44] J. McDougall and E. C. Stoner, Phil. Trans. Roy. Soc. London **A237**, 9 (1938).
[45] R. B. Dingle, Appl. Sci. Res. **B6**, 225 (1957).

where σ is the total conductivity, p_1 is the number of holes in band 1, p_2 is the number in band 2, μ_1 and μ_2 are the mobilities of the corresponding bands, and e is the electronic charge. For the pure dilatational strain resulting from the application of hydrostatic pressure it can be shown from the tensor relationships described above that

$$(m_{11}+2m_{12})/3=\mathrm{d}\ \ln\sigma/d\ \ln V, \tag{10}$$

where V is the volume. Letting the mobilities of the two bands be independent of strain, from Eqs. (4), (9), and (10) we obtain

$$\frac{m_{11}+2m_{12}}{3}=\frac{E_2}{kT}\frac{1-b}{1+\alpha b}\times\left\{\frac{\alpha\mathfrak{F}_{-1/2}(\eta_2)\mathfrak{F}_{1/2}(\eta_1)}{1+\alpha[\mathfrak{F}_{-1/2}(\eta_2)/\mathfrak{F}_{1/2}(\eta_2)][\mathfrak{F}_{1/2}(\eta_1)/\mathfrak{F}_{-1/2}(\eta_1)]}\right\}, \tag{11}$$

when Fermi-Dirac statistics are applied to both bands. $E_2=d\Delta/d\ \ln V$ is the deformation potential of the energy gap Δ between the bands; b is the mobility ratio μ_2/μ_1; $\alpha=X/1-X$, where X is the fractional number of carriers in the second band, and η_2 and η_1 give the position of the Fermi level in units of kT relative to each band edge. When the statistics are classical in both bands, Eq. (11) simplifies to

$$\frac{m_{11}+2m_{12}}{3}=\frac{E_2}{kT}\frac{(1-b)X}{1+(X/1-X)b}. \tag{12}$$

Analogous to the mobility anisotropy K in a single multivalley band, the mobility ratio b determines the change in the average transport properties when carriers are transferred between bands. Unlike the situation in a multivalley band, $(m_{11}+2m_{12})/3$ decreases with decreasing temperature because of an exponential decrease in X.

2. *Strain-Dependent Effective Mass*

Another large contribution to π_H occurs even in a single-band extrinsic semiconductor when the effective mass is strain-dependent. This will be the case for example when the energy gaps between the conducting band and those bands with which it interacts are small.[34,46] Although an adequate theory to describe the scattering processes in PbTe is not avialable, the temperature dependence of the mobility[28] shows that acoustic-mode scattering is important. To obtain an estimate of the elastoconductance resulting from the change in effective mass produced by pure dilatation, we have used the deformation-potential formulation of the mobility for scattering by long-wavelength longitudinal acoustic modes.[47] For ellipsoidal energy surfaces and Fermi-Dirac statistics, this is given by

$$\mu=C\frac{1}{(m_Tm_Tm_L)^{1/2}}\frac{1}{3}\left(\frac{1}{m_L}+\frac{2}{m_T}\right)\frac{\mathfrak{F}_0(\eta)}{\mathfrak{F}_{1/2}(\eta)}, \tag{13}$$

where C is a constant independent of m_T, m_L, and η. Band-structure calculations by Lin and Kleinman[48] and Shubnikov–de Haas measurements by Cuff *et al.*,[15] show that to a good approximation only the transverse mass m_T is sensitive to the energy gap E_G between the principal valence and conduction bands and that $m_T\propto E_G$. Using Eqs. (4), (10), and (13) and the proportionality between m_T and E_G, we obtain

$$\frac{m_{11}+2m_{12}}{3}=-\left(1+\frac{2K_m}{2K_m+1}\right)\frac{E_1}{E_G}+\left(1-\frac{\mathfrak{F}_{-1}(\eta)}{\mathfrak{F}_0(\eta)}\frac{\mathfrak{F}_{1/2}(\eta)}{\mathfrak{F}_{-1/2}(\eta)}\right)\frac{E_1}{E_G}. \tag{14}$$

$E_1=dE_G/d\ \ln V$, the deformation potential of the energy gap E_G and $K_m=m_L/m_T$, the mass ratio. For classical statistics, the second term on the right vanishes.

III. EXPERIMENTAL

The geometry of the samples and the crystallographic orientations of stress and current that were used are shown in Fig. 3. The samples were cut from slices oriented to 0.5° or better by means of optical reflection from a cleaved surface. They were then ground to final dimensions of 0.30×0.40×0.300 in. An exception to this procedure, for some of the samples on which transverse measurements were made, will be described below. Current and resistivity probes were attached to the sample by discharging a 300 μF condensor charged to 18 V across the contact. Platinum wires, 0.002 in. in diameter, were used.

When the sample current is independent of the applied stress (a condition which was met by placing a large resistor in series with the sample), it can be shown[35] that

$$\frac{1}{X}\frac{\Delta E_J}{E_J}=\pi_{12}+(\pi_{11}-\pi_{12}-\pi_{44})\sum_{i=1}^{3}\alpha_i^2\beta_i^2+\pi_{44}\cos^2\theta, \tag{15}$$

where X is the applied-uniaxial stress, E_J is the component of the electric field in the current direction, ΔE_J is the change in this component due to the stress, α_i and β_i are, respectively, the direction cosines of the current and stress with respect to the cubic axes, and θ is the angle between the current and stress. The piezoresistance coefficients were determined primarily by measurements using configurations (a), (b), and (c)

[46] H. Jones, *The Theory of Brillouin Zones and Electronic States in Solids* (North-Holland Publishing Company, Amsterdam, 1962), p. 42.

[47] W. Shockley and J. Bardeen, Phys. Rev. **77**, 407 (1949).

[48] P. J. Lin and L. Kleinman, Phys. Rev. **142**, 478 (1966).

shown in Fig. 3. Configuration (d) was sometimes used as a consistency check on the results. Assuming that the current lines between the resistivity probes are parallel to the long dimension of the sample, we have[35]

$$\pi_{11}=\frac{1}{X}\frac{\Delta V}{V}+(S_{11}-2S_{12}),$$

$$\pi_{12}=\frac{1}{X}\frac{\Delta V}{V}-S_{11},$$

and

$$\tfrac{1}{2}(\pi_{11}+\pi_{12}+\pi_{44})=\frac{1}{X}\frac{\Delta V}{V}+\left(\frac{S_{44}}{2}-S_{12}\right), \quad (16)$$

for configurations (a), (b), and (c), respectively. $\Delta V/V$ is the fractional change in the voltage between the resistivity probes. The terms containing the compliance constants S_{ij} correct for changes in the sample dimensions.

A. Apparatus

For longitudinal measurements, in which the stress is parallel to the current, the apparatus shown in Fig. 4 was used to apply the stress. The sample is held in place and the stress applied to it by the thin-walled stainless steel tube. Such a tube minimizes heat flow to the sample during measurements below room temperature. Good thermal stability requires that the contact between the sample and tube be maintained throughout the measurement. Using this arrangement,

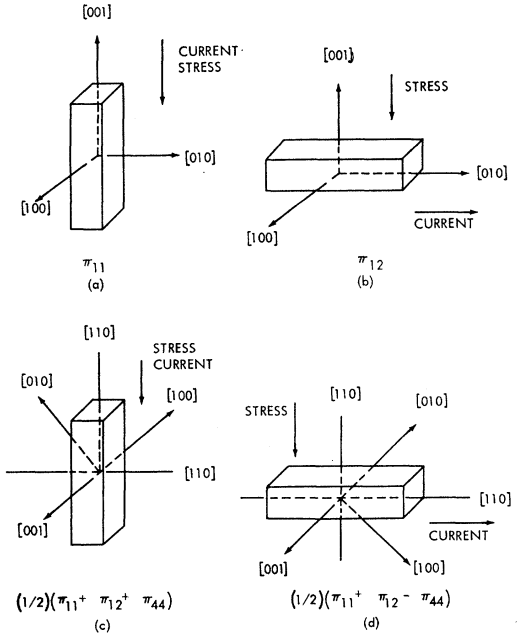

FIG. 3. Sample geometry and crystallographic orientations of the stress and current.

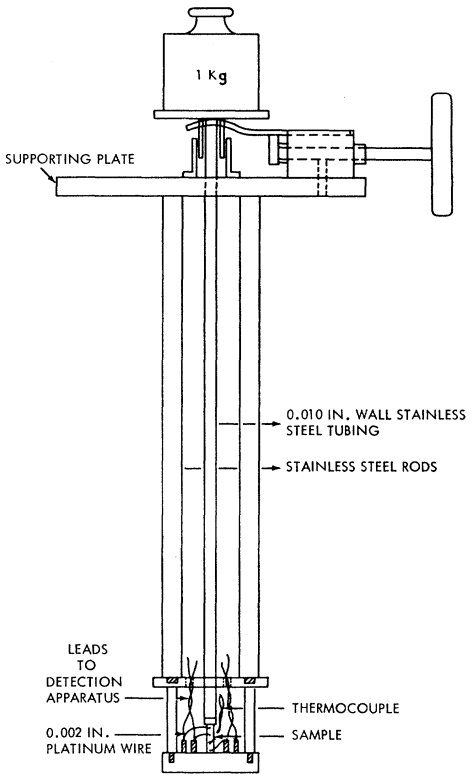

FIG. 4. Apparatus used to apply the stress.

some samples were subjected to stresses as high as 1×10^8 dyn/cm^2.

Transverse measurements, in which the stress is perpendicular to the current, are difficult to make. A number of workers[30,38,49] have done this by attaching long current electrodes to the sides of the sample as shown in (a) of Fig. 5. In situations where this technique works, corrections must be made for the curvature of the current lines near the ends of the electrodes. We attempted to use this method also, but our resistivity measurements indicated that the current lines were not distributed uniformly between the electrodes. We suspect this was due to the low resistivity of p-PbTe which makes it difficult to obtain large electrodes with resistance negligible to that across the sample. This hypothesis was substantiated by attaching thicker electrodes after which the measured resistivity was in closer agreement with the value obtained by the conventional method. This was not pursued further because of the shear stresses set up by thick electrodes when the stress is applied. Instead, the arrangement shown in (b) of Fig. 5 was used with the apparatus shown in Fig. 4. This technique suffers from a difficulty also, that of applying a uniform stress over a large area. To accomplish this, the whole assembly was constructed of quartz which provides an electrically insulating material

[49] R. F. Potter, Phys. Rev. 108, 652 (1957).

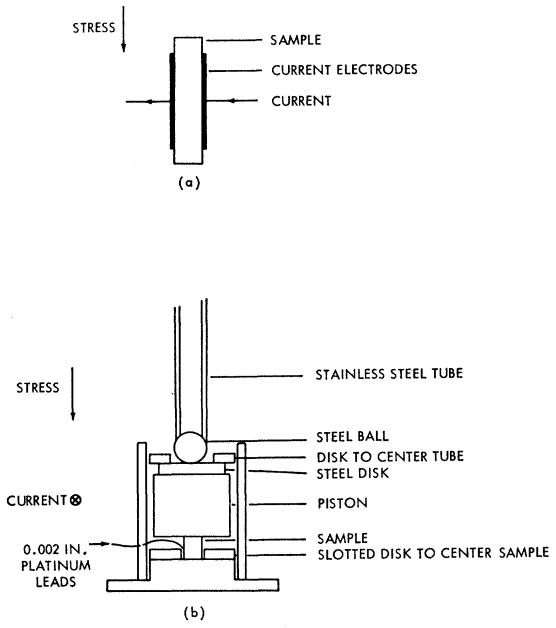

FIG. 5. Two methods for making transverse measurements. Method (b) used for the results reported in this paper.

in which precise tolerances can be held over a large temperature range because of its low thermal coefficient of expansion. The slot in the lower disk was made 0.001 in. larger than the sample width, and the hole in the upper disk was 0.001 in. larger than the outside diameter of the stainless steel tube. The two disks were centered by the outer cylinder. Because the diameter of the tube is much larger than the width of the sample, a steel ball was inserted under the tube in order to locate the point of application of the force over the center of the sample. Samples on which these measurements were to be made were very carefully ground so that the top and bottom faces would be parallel. In addition, some samples were polished optically flat and parallel. In spite of all these precautions, it was not always possible to obtain reliable results. When the resistivity change was proportional to the stress, we assumed that the stress was being applied uniformly. Because of the larger area across which the stress was being applied in the transverse measurements, it was not convenient to apply stresses larger than about 2.5×10^7 dyn/cm^2.

Hydrostatic pressure measurements were made near room temperature up to somewhat less than 2000 atm. The pressure was generated by a Blackhawk hand pump using a light oil as the pressure transmitting medium. The pressure was measured by a Heine gauge which yielded values accurate to 0.5%. The sample temperature was kept constant by immersing the vessel in a well regulated water bath.

B. Detection Equipment

Our first results were obtained by passing a dc current through the sample and measuring the voltage change produced by the stress on a millimicrovoltmeter after bucking out the zero-stress voltage with a potentiometer. Currents less than 100 mA were used. For these currents, the voltage drop between the resistivity probes was in the microvolt or low millivolt range depending on the carrier concentration and temperature of the sample. For stresses that could be applied conveniently, the voltage change was sometimes less than a microvolt and sometimes as high as tens of microvolts. Because of these low level signals, the measurements were impaired by a strain-induced change in the thermal emf between the resistivity probes that was set up by Peltier heating and cooling at the current contacts. To eliminate this, a 37.5 cycles/sec chopped dc current was used. Calculations showed that at this frequency the resulting temperature wave, produced by the Peltier effect, was damped out before reaching the resistivity probes. The chopped current was provided by a 6-V battery and a mechanically driven double-pole double-throw switch which was one of a set of four low-contact emf (<0.02 μV) switches manufactured by Guildline Instruments. The resistivity voltage was then demodulated by adjusting the phase of a second switch relative to the first. A test circuit was designed so that this phase relationship could be precisely set by observing both waveforms simultaneously on a dual-beam oscilliscope. Figure 6 is a block diagram of the complete detection system.

C. Cryostat

The cryostat used for the measurements was very simple. From room temperature down to about 100°K, the sample was cooled in a 4-liter Dewar containing 2-methylbutane. To obtain data at any desired tempera-

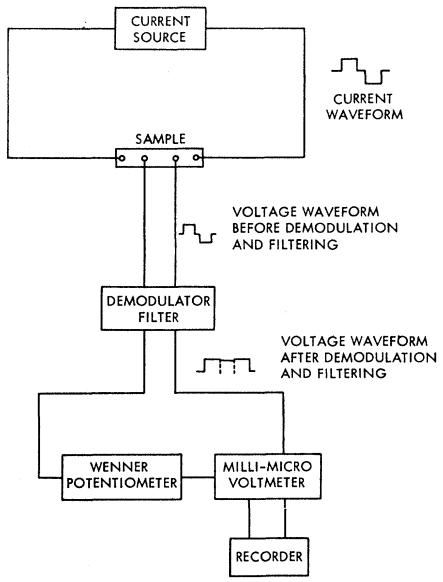

FIG. 6. Block diagram of detection apparatus.

ture in this range, liquid nitrogen was pumped through a glass coil in the bath by means of compressed nitrogen gas. When the temperature at the thermocouple was about 8°K above the desired value, the flow of nitrogen was stopped. The cooler liquid near the coil would then equilibriate the bath at the lower temperature. During a set of about five repreated measurements, the temperature drift at the thermocouple next to the sample was less than 0.5°K.

A measurement at 77°K was made by direct immersion in liquid nitrogen. This was very difficult when dc currents were first used because of voltage fluctuations produced by the bubbling nitrogen. However, when the chopped dc current was used, these fluctuations turned out to be much smaller and were not bothersome.

IV. RESULTS AND DISCUSSION

All of the samples that were measured were taken from crystals grown by the Czochralski technique. These crystals had no low-angle grain boundaries and a dislocation density of $10^5/cm^2$ or less. The properties of these samples are listed in Table I. The as-pulled crystals had a carrier concentration of about 3.5×10^{18} cm^{-3}. Lower concentrations were obtained by annealing at temperatures lower than the pull temperature. This method for obtaining a range of concentrations in PbTe was first explored by Scanlon.[50] A detailed description of the sample treatment for the work reported here is given in Ref. 35. The two samples with the highest concentrations were obtained by sodium doping. The quoted values of the carrier concentration were obtained

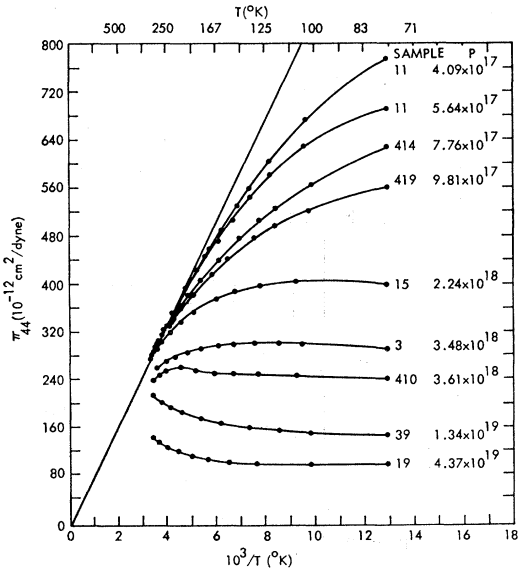

FIG. 7. Temperature dependence of π_{44} as a function of hole concentration.

[50] W. W. Scanlon, Phys. Rev. **126**, 509 (1962).

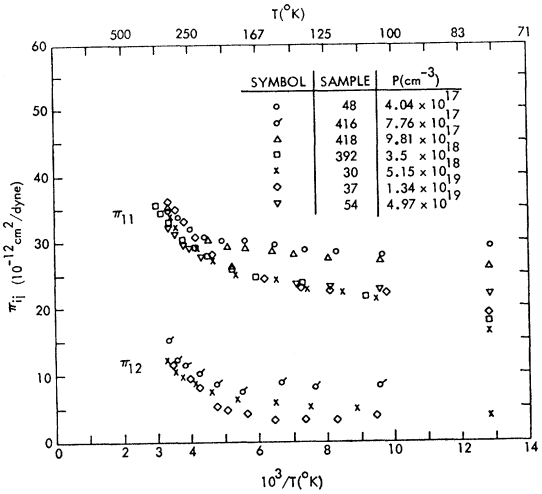

FIG. 8. Temperature dependence of π_{11} and π_{12} as a function of hole concentration.

from the formula

$$p=1/R_{77°K}e, \tag{17}$$

where p is the hole concentration, $R_{77°K}$ is the weak-field Hall coefficient in cm^3/coulomb measured at 77°K, and e is the electronic charge in coulombs. This relationship was used to standardize the carrier concentrations of the samples for two reasons. First, the actual relationship between R and p in a multivalley band involves the mass ratio of the ellipsoids. This is a function of p and not known in detail. Second, at temperatures above 200°K a second valence band becomes populated. This requires a more complicated relationship between p and R.

Figures 7 and 8 show the temperature dependence of the three piezoresistance coefficients of the valence band of PbTe for the range of carrier concentrations provided by the samples listed in Table I. The values of π_{44} have been corrected for the dimensional changes produced by the stress by use of the compliance constants. This correction is less than 2% of the room-temperature value and decreases in magnitude at lower temperatures. The values of π_{11} and π_{12} have not been corrected because we will be interested in combinations of these coefficients for which the corrections are unimportant for our purposes. Values for the elastic and compliance constants of PbTe at 303 and 77°K are given in Table II.

A. π_{44}

1. Temperature Dependence

The behavior of the data in Fig. 7 is clearly in agreement with what is expected from the carrier transfer effect in a ⟨111⟩ multivalley band. We notice first that as the carrier concentration is lowered and the statistics are classical over a greater temperature range, more and more of the data exhibit the $1/T$ temperature de-

TABLE I. Properties of the p-type PbTe samples studied.

Sample No.	Crystal No.	Sample orientation	Hole conc. (cm^{-3})	Hall coeff. (cm^3/C) Room temp.	Hall coeff. (cm^3/C) 77°K	$R_{298°K}/R_{77°K}$	Resistivity (10^{-3} Ω cm) Room temp.	Resistivity (10^{-3} Ω cm) 77°K	Hall mobility (cm^2/V sec) Room temp.	Hall mobility (cm^2/V sec) 77°K
405	18A	Unorien.	3.45×10^{17}							
411	18A	Unorien.	3.70×10^{17}	18.8	16.9	1.111	26.3	0.852	714	18 800
48	1H	[100]	4.04×10^{17}	19.5	15.5	1.258	22.6	0.587	866	26 300
11	7A	[110]	4.09×10^{17}	18.8	15.3	1.229	21.3	0.559	882	27 400
11[a]	7A	[110]	5.64×10^{17}	13.7	11.1	1.233	16.1	0.435	852	24 400
416	2B	[100]	7.54×10^{17}	10.5	8.31	1.264	11.5	0.339	921	24 500
414	2B	[110]	7.76×10^{17}	10.2	8.05	1.268	11.6	0.322	893	24 900
418	2B	[100]	9.81×10^{17}	7.73	6.37	1.211	8.59	0.257	900	24 800
419	2B	[110]	9.8×10^{17}					0.261		
15	7A	[110]	2.24×10^{18}	3.88	2.79	1.390	3.95	0.128	985	21 800
3	7A	[110]	3.48×10^{18}	2.48	1.79	1.386	2.85	0.114	868	15 700
392	12	[100]	2.5×10^{18}					0.137		
397	12	[100]	3.5×10^{18}					0.128		
184	16	[100]	3.5×10^{18}							
410	2	[110]	3.61×10^{18}	2.39	1.73	1.382	2.74	0.114	871	15 200
380	2/26/59	Unorien.	4.05×10^{18}	2.12	1.55	1.369	2.30	0.0927	924	16 700
30	1H	[100]	5.15×10^{18}	1.73	1.21	1.430	2.03	0.0918	931	14 200
39	1H	[110]	1.34×10^{19}	0.732	0.468	1.565	0.751	0.0566	974	8 270
37	1H	[100]	1.34×10^{19}					0.0565		
19	4Na	[110]	4.37×10^{19}	0.278	0.143	1.945	0.448	0.0558	622	2 560
54	5Na	[100]	4.97×10^{19}	0.235	0.126	1.865	0.387	0.0526	608	2 400

[a] Annealed at higher temperature.

pendence described by Eq. (6), the classical limit of Eq. (1). On the other hand, for the higher-concentration samples, there is a temperature range over which π_{44} is approximately temperature-independent. This is consistent with Eq. (7), the degenerate limit approximation to Eq. (1).

In the temperature range where $\pi_{44} \propto 1/T$, Eq. (6) can be used to calculate a value for the shear deformation potential Ξ_u, independent of a choice of the scattering index s, if the mobility anisotropy factor K has been determined independent of s. From magnetoresistance measurements at 298 and 77°K on samples with $p \approx 3.5\times10^{18}$ cm^{-3}, Allgaier[10] obtained K values of 4.74 and 4.20, respectively. For samples with this p, it can be shown[10] that $K_{298°K}$ depends upon s, while $K_{77°K}$ does not. Since K is temperature-insensitive and the factor $(K-1)/(2K+1)$ in Eq. (6) is K-insensitive, we have chosen to use $K_{77°K}$ in our computation of Ξ_u. Then, using π_{44}(298°K), we obtain the value 8.5 eV for Ξ_u. From a theoretical calculation of the effect of strain on the band structure of PbTe, Ferreira[51] has obtained the value 10.5 eV.

TABLE II. Elastic and compliance constants of p-type PbTe at 303 and 77°K.[a]

Temp. (°K)	Elastic constants (10^{11} dyn/cm²) C_{11}	C_{12}	C_{44}	Compliance constants (10^{-12} cm^2/dyn) S_{11}	S_{12}	S_{44}
303	10.80	0.76	1.345	0.937	−0.061	7.436
77	12.38	0.46	1.475	0.089	−0.029	6.779

[a] R. E. Strakna and A. E. Clark (private communication).

[51] L. G. Ferreira, Phys. Rev. **137**, A1601 (1965).

Using Eq. (1) and $\Xi_u = 8.5$ eV, the temperature dependence of π_{44} between 298 and 77°K was calculated for $p = 4.09\times10^{17}$ cm^{-3}. A linear interpolation between $K_{298°K}$ and $K_{77°K}$ was assumed. The temperature dependence of η was deduced from Eq. (4) and the temperature dependence of the density-of-states mass m_D obtained from the thermoelectric power measurements of Cuff, Ellett, and Kuglin.[15] In order to calculate the η dependence of the F-D factor, a value for the scattering index s must be chosen. Based on the work of Vinogradova *et al.*,[27] Cuff, Ellett, and Kuglin,[15] and Allgaier and Houston,[28] the best choice is $s = -\frac{1}{2}$, appropriate for one-phonon acoustic mode scattering. The results of the calculation are compared with the experimental values in Fig. 9. We now consider some of the possible causes for the discrepancy.

Nonparabolicity of the valence band has been reported.[15,16,21] However, the effect is negligible at this p and in a later section we show that, for degenerate statistics at least, π_{44} is reduced rather than enhanced by the nonparabolicity.

If the deformation potential were strongly temperature-dependent, it is unlikely that there would be a temperature range over which the $1/T$ behavior of π_{44} would be observed.

Equation (1) assumes only intravalley scattering. Intervalley scattering can also be important in a multivalley semiconductor. The effect of this scattering mechanism on the piezoresistance has been considered by Herring,[39] Herring and Vogt,[40] and Keyes.[34] They show that for classical statistics, intervalley scattering leads to a deviation of π_{44} from the $1/T$ dependence for temperatures in the range $0.5\ T_D \leq T \leq 2T_D$, where T_D is the Debye temperature. T_D for PbTe is about 140°K

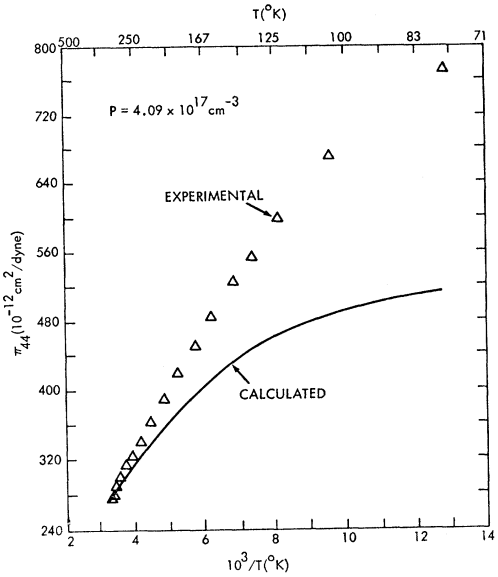

FIG. 9. Calculated and experimental temperature dependence of π_{44} for $p=4.09\times10^{17}$ cm^{-3}.

(Ref. 52). Since π_{44} is a linear function of $1/T$ down to about 160°K, it does not appear that any significant amount of intervalley scattering is present below room temperature.

Evidence for the population of a second valence band is presented in a later section of this paper. However, even at room temperature for $p=4.09\times10^{17}$ cm^{-3}, only about 20% of the carriers are in this band, and this percentage decreases as the temperature decreases. The complete inadequacy of these considerations indicates the need for a radical modification of either the band parameters used in the calculation or the theory of the carrier-transfer effect when applied to PbTe. The former seems more likely because, for example, recent neutron-diffraction results[53] on PbTe have shown that the phonon spectrum is so complicated that it would be surprising if any given scattering mechanism were to predominate over the temperature range we have investigated.

The behavior of the two samples with the highest concentrations is interesting because π_{44} decreases as the temperature is lowered even though these samples are degenerate throughout the entire temperature range. One explanation for this, suggested by Eq. (7), is that the Fermi level E_F is increasing. This would be consistent with the reported temperature dependence of the density-of-states hole mass m_D [15] and the electric-susceptibility hole mass m_S.[21,54] These masses decrease as the temperature is lowered thus decreasing the density of states. The two curves also appear to level off at the lower temperatures. Since m_D continues to decrease down to at least 4.2°K, (Ref. 15), the leveling off must be attributed to another mechanism. This will be considered in more detail in the next section.

2. Carrier-Concentration Dependence

It is more convenient in PbTe to consider the carrier-concentration dependence of π_{44} at a fixed temperature. Calculations are somewhat simplified because it is no longer necessary to consider the strong temperature dependence of the band parameters. Figure 10 shows the dependence of π_{44} on hole concentration for several of the temperatures at which the measurements were made. The over-all behavior is that the higher the temperature, the greater is the range of p over which π_{44} is independent of p. In this range, the statistics are classsical. For higher p values, π_{44} decreases because of the decrease in the F-D factor which occurs with the departure from classical statistics.

We were most interested in the carrier-concentration dependence at 77°K for purposes of investigating the nonparabolic nature of the band. The theory for a single parabolic band predicts a simple dependence of π_{44} on p. For completely degenerate statistics, Eq. (4) can be written

$$E_F=(3/\pi)^{2/3}(h^2/8m_D)p^{2/3}. \tag{18}$$

Substituting Eq. (18) into Eq. (7), we obtain

$$\pi_{44}=\frac{\Xi_u}{3C_{44}}\left[\frac{K-1}{2K+1}\frac{s+\frac{3}{2}}{(3/\pi)^{2/3}(h^2/8m_D)}\right]p^{-2/3}. \tag{19}$$

Thus, if the parameters inside the square brackets are independent of p, a log-log plot of π_{44} versus p should have a slope equal to $-\frac{2}{3}$ over the range of p for which the statistics are degenerate. The carrier-concentration dependence of π_{44} at 77°K is replotted in Fig. 11, and indicated by the circles. The solid line is the result of a calculation using Eq. (1) and the parameters

$$\begin{aligned} K&=4.20,\\ m_L&=0.31,\\ m_T(0)&=0.038,\\ s&=-\tfrac{1}{2}. \end{aligned} \tag{20}$$

The values $m_L=0.31$ and $m_T(0)=0.022$ at 4.2°K have been reported by Cuff *et al.*[16] $m_T(0)=0.038$ at 77°K was obtained from Eq. (3a) of Ref. 16 and the temperature dependence of the gap between the valence and conduction bands. The experimental values of π_{44} are a factor of 2 larger than the calculated values at low concentrations where the parabolic band approximation should be quite good. A density-of-states mass of 0.39 is needed to obtain agreement. This is more than twice the value previously reported.[15] Focusing attention now on the carrier-concentration behavior, we see that although the statistics are certainly degenerate for $p>6$

[52] D. H. Parkinson and J. E. Quarrington, Proc. Phys. Soc. (London), **A67**, 569 (1954).
[53] W. Cochran, R. A. Cowley, G. Dolling, and M. M. Elcombe, Proc. Roy. Soc. (London) **A293**, 433 (1966).
[54] H. A. Lyden, Phys. Rev. **135**, A514 (1964).

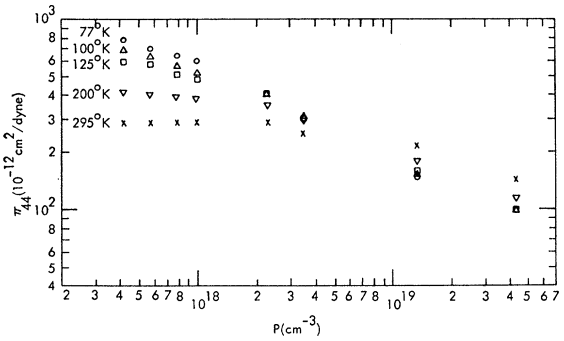

FIG. 10. Hole-concentration dependence of π_{44} at several temperatures.

$\times 10^{18}$ cm^{-3}, the data do not exhibit the $-\frac{2}{3}$ slope predicted by Eq. (19) for this range. Cuff *et al.*[15,16] have observed an increase in m_T with increasing carrier concentrations while Dixon and Riedl[21] have observed a similar behavior in the electric susceptibility mass m_S. They have successfully interpreted their results on the basis of a dispersion relationship proposed by Cohen[55] for extrema at the L points of the Brillouin zone in bismuth. In this model, only one of the masses is energy-dependent. According to Eq. (1), an increase of m_T with p will result in a decrease in both $\eta(=E_F/kT)$ and $K[=\mu_T/\mu_L=(m_L/m_T)(\tau_T/\tau_L)]$ relative to their values for the same p in a parabolic band. τ_T/τ_L is the relaxation-time anisotropy. Since these effects tend to compensate for one another, the net result could either be an increase or a decrease in π_{44} relative to values in a parabolic band. Using the Cohen relationship

$$E=\frac{\hbar^2}{2}\left\{\frac{k_T^2}{m_T(0)[1+(1/E_G)(E+\hbar^2k_L^2/2m_L')]}+\frac{k_L^2}{m_L}\right\}, \tag{21}$$

where k_T and k_L are, respectively, wave vectors perpendicular and parallel to a $\langle 111\rangle$ direction, E_G is the energy gap between the conduction and valence band, and m_L' is the longitudinal mass of the conduction band, new expressions for the components of the conductivity tensor were derived. The procedure for calculating π_{44} is then the same as for a parabolic band. The details are given in Ref. 35. For Fermi-Dirac statistics, the result involves integrals over energy which have not been tabulated. However, in the limit of degenerate statistics, the integrals reduce to the values of the integrand at the Fermi surface and the result is simplified. We obtained

$$\pi_{44}=\frac{\Xi_u}{3C_{44}}\frac{K-1}{2K+1}\frac{s+\frac{3}{2}}{E_F}\times\left\{\frac{1-f(E_F/E_G)K+g(E_F/E_G)}{K-1}\right\}, \tag{22a}$$

where

$$K=\frac{m_L}{m_T(0)}\frac{\tau_T}{\tau_L}\frac{1+(6/5)E_F/E_G}{1+(12/5)E_F/E_G+(12/7)(E_F/E_G)^2} \tag{22b}$$

and

$$f(E_F/E_G)=\frac{(4/5)E_F/E_G}{(1+2E_F/E_G)[1+(6/5)E_F/E_G]},$$

$$g(E_F/E_G)=\frac{(2/5)E_F/E_G+(24/7)(E_F/E_G)^2+(24/7)(E_F/E_G)^3}{(1+2E_F/E_G)[1+(12/5)E_F/E_G+(12/7)(E_F/E_G)^2]}. \tag{22c}$$

Equation (22a) reduces to Eq. (7) ,the expression for a parabolic band, as the ratio E_F/E_G goes to zero.

The relationship between the carrier concentration and the Fermi level for this band model, analogous to Eq. (4), is given by

$$p=2[2\pi m_D(0)kT/h^2]^{3/2}[\mathfrak{F}_{1/2}(\eta)+(3kT/E_G)\mathfrak{F}_{3/2}(\eta)], \tag{23}$$

where $m_D(0)$ is the density-of-states mass at the band edge. Using Eqs. (20), (22) and (23), and assuming an isotropic relaxation time ($\tau_T/\tau_L=1$), π_{44} was calculated for several values of p. The results, indicated by the dashed line in Fig. 11, show that π_{44} is smaller than calculations for a parabolic band would indicate and therefore cannot explain the relative increase in π_{44} at high p. This increase can however be explained on the basis of an increase in the scattering index s. The deviation from a $p^{-2/3}$ behavior appears to begin with a p of about 6×10^{18} cm^{-3} which is in the concentration range where the Hall mobility at 77°K starts to drop off rapidly.[28] The dropoff in Hall mobility has been attributed to the onset of scattering from defects produced by deviations from stoichiometry.[28] These defects behave like neutral impurities[27,28] because of the large dielectric constant in PbTe. Vinogradova *et al.*[27] have shown that this type of scattering in PbTe results

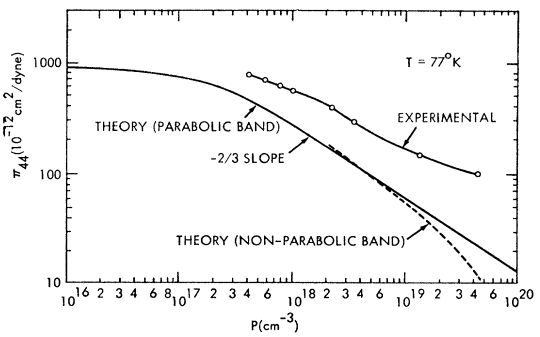

FIG. 11. Calculated and experimental hole-concentration dependence of π_{44} at 77°K.

[55] M. H. Cohen, Phys. Rev. **121**, 387 (1961).

in a relaxation time which is energy-independent ($s=0$). Thus a trend toward a larger s value at high p is reasonable.

B. $\pi_{11}+2\pi_{12}$

1. Temperature Dependence

The temperature dependence of the hydrostatic piezoresistance coefficient $\pi_{11}+2\pi_{12}$ for several carrier concentrations is shown in Fig. 12. As discussed earlier, these values were computed from the individual measurements of π_{11} and π_{12}. $\pi_{11}+2\pi_{12}$ was also obtained from the low-pressure region of hydrostatic pressure measurements made on samples having the carrier concentration $p\approx 3.5\times 10^{18}$ cm^{-3}. The pressure dependence of the fractional change in resistance of these samples at two temperatures near room temperature is shown in Fig. 13. The values of $\pi_{11}+2\pi_{12}$ obtained from the hydrostatic measurements are in good agreement with the values computed from the individual measurements of π_{11} and π_{12}. We mentioned earlier that π_{12} is difficult to measure. The agreement between the two methods indicates that the values of π_{12} are reliable.

The observed values of $\pi_{11}+2\pi_{12}$ are probably much larger than what is expected from the pressure dependence of the phonon spectrum. In spite of the complications of this spectrum, it is interesting to obtain an estimate of this effect for a lattice of independent harmonic osicllators from the Gruneisen constant[56]

$$\gamma=-\frac{d\ln\nu}{d\ln V}=\frac{\alpha V_0}{\chi_0 C_v}, \tag{24}$$

where ν is the frequency of a normal mode, α is the thermal expansion coefficient, V_0 and χ_0 are, respectively, the specific volume and compressibility at 0°K,

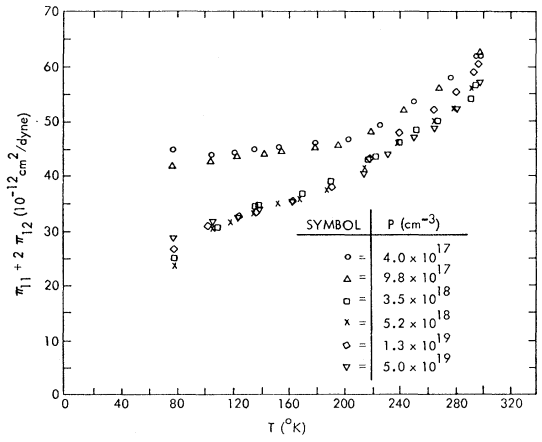

FIG. 12. Temperature dependence of $\pi_{11}+2\pi_{12}$ for a range of hole concentrations.

[56] N. F. Mott and H. Jones, *Theory of the Properties of Metals and Alloys* (Dover Publishing Company, New York, 1958), p. 19.

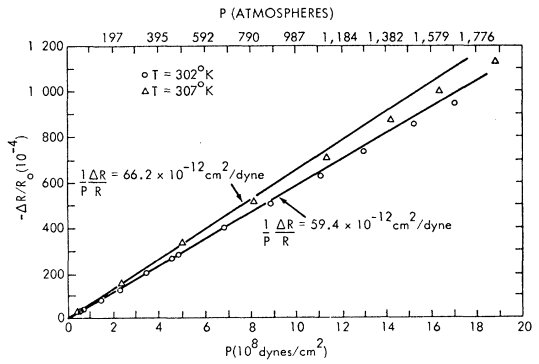

FIG. 13. Pressure dependence of the fractional change in resistance at 302 and 307°K for samples with a hole concentration of about 3.5×10^{18} cm^{-3}.

and C_v is the specific heat at constant volume. It can be shown[57] that

$$\frac{d\ln\nu}{d\ln v}=\frac{1}{2}\frac{d\ln\sigma}{d\ln V}=\frac{1}{2}\frac{m_{11}+2m_{12}}{3}. \tag{25}$$

Therefore, from the relationship between elastoconductance and piezoresistance, and Eqs. (24) and (25),

$$\pi_{11}+2\pi_{12}=-\frac{(m_{11}+2m_{12})/3}{(C_{11}+2C_{12})/3}=\frac{2\gamma}{(C_{11}+2C_{12})/3}. \tag{26}$$

Using reported values of the parameters in Eq. (24), $\pi_{11}+2\pi_{12}=4.3\times 10^{12}$ cm^2/dyn at 300°K, an order of magnitude smaller than the observed values.

Using Eq. (14), the elastoconductance based on the volume dependence of the transverse effective mass m_T, the temperature dependence of $(m_{11}+2m_{12})/3$ between 77 and 298°K was calculated for $p=4.0\times 10^{17}$ cm^{-3}. The lowest concentration was chosen so that effects due to nonparabolicity of the band would not be important. The temperature dependence of the energy gap E_G between the valence and conduction bands and the temperature dependence of the deformation potential E_1 were obtained by linear interpolation between the reported values (Refs. 1, 3, 24, and 3, respectively)

$$\begin{aligned} &E_G(300°\text{K})=0.32\text{ eV},\\ &E_G(\ 77°\text{K})=0.217\text{ eV},\\ &E_1(300°\text{K})=2.8\text{ eV},\\ &E_1\ (77°\text{K})=2.1\text{ eV}. \end{aligned} \tag{27}$$

As before, the temperature dependence of E_G was used in conjunction with Eq. (3a) of Ref. 16 in computing η and K_m. The results of the calculation and the contribution 2γ, which has been assumed to be temperature-independent, are given by the solid line in Fig. 14. The circles were obtained from the experimental values

[57] See Ref. 56, pp. 244 and 271.

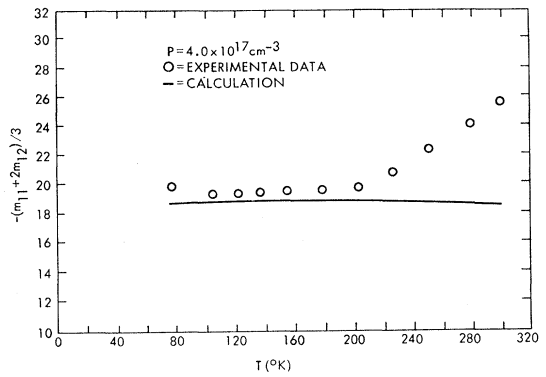

FIG. 14. Comparison of the observed temperature dependence of the elastoconductivity produced by a pure dilatation with that calculated from the strain dependence of the effective mass of the ⟨111⟩ band. The calculation includes the contribution 2γ.

of $\pi_{11}+2\pi_{12}$ for this concentration, the relationship between the elastoconductivity and piezoresistance given by the first two terms in Eq. (26), and the temperature dependence of the elastic constants.[58] The agreement at the low-temperature end is remarkably good. Although this may be fortuitous because the mobility formulation on which the calculation is based is probably an oversimplification, it strongly suggests that the large values of $\pi_{11}+2\pi_{12}$ occurring between 77°K and 200°K are the result of the pressure dependence of the transverse mass m_T.

The sharp rise in $(m_{11}+2m_{12})/3$ beginning at 200°K suggests that an additional mechanism for elastoconductivity becomes important above this temperature. Allgaier[22] and Allgaier and Houston[23] find that the Hall coefficient also starts to increase at about 200°K for samples with this concentration. The total increase from a constant low-temperature value to the value at 300°K [see $R(300°K)/R(77°K)$ in Table I] is much more than can be accounted for by a single-band expression for the Hall coefficient. Equation (12) gives the elastoconductivity resulting from the transfer of carriers between two bands when pressure changes the energy gap between them. This expression, appropriate for classical statistics, is a good approximation to Eq. (11) above 200°K for $p=4.0\times10^{17}$ cm^{-3}. Allgaier[22] has estimated the mobility ratio $b=\mu_2/\mu_1$ of the two bands to be about 0.1. The ratio of the Hall coefficient at a temperature T at which two-band conduction takes place to the Hall coefficient at a temperature T_0 at which there are carriers in one band only can be accurately written

$$\frac{R(T)}{R(T_0)}=\frac{(1-X)+Xb^2}{[(1-X)+Xb]^2}, \tag{28}$$

where $X=p_2/p$ is the fractional number of carriers in band 2. For $p=4.0\times10^{17}$ cm^{-3}, $R(298°K)/R(77°K)=1.24$. Using $b=0.1$ and solving Eq. (28), we obtain $X=0.24$, that is 24% of the carriers are in the second band at 298°K. Therefore, the deformation potential E_2 of the gap between the two valence bands can be determined from Eq. (12) if the elastoconductance resulting from two-band conduction is known. Because of the uncertainties involved in a calculation of the absolute value of the pressure-induced elastoconductivity in the ⟨111⟩ band, we have assumed that the two-band contribution to $(m_{11}+2m_{12})/3$ is equal to the difference between the data at 298°K and the extrapolation of the low-temperature plateau. From this assumption we obtain $E_2=-1.0$ eV. The value of E_2 corresponding to the pressure coefficient of the gap reported by Sato, Fujimoto, and Kobayshi[24] is -2.5 eV. Their calculations however, are based on a much larger mobility ratio.

2. *Carrier-Concentration Dependence*

The carrier-concentration dependence of $\pi_{11}+2\pi_{12}$ at 77°K is plotted in Fig. 15. The decreasing values at low p are consistent with an energy-dependent transverse mass m_T which increases as the Fermi level increases. Consideration of the expression for the transverse mass m_T in a nonparabolic band given by Eqs. (3a) and (3b) of Ref. 16, reveals that for values of the Fermi level comparable to the energy gap between the ⟨111⟩ conduction and valence bands, the important energy term in the expression for the transverse mass m_T is E_G+2E_F, where E_F is the Fermi level with respect to the valence-band maximum. (See insert in Fig. 15.) If we replace E_G in Eq. (14) by E_G+2E_F as a first-order correction to the parabolic band expression, we can see that as the hole concentration is increased, $\pi_{11}+2\pi_{12}$ should decrease.

The minimum in $\pi_{11}+2\pi_{12}$ near $p=4\times10^{18}$ cm^{-3} is surprising. One would expect the decrease to continue at a decreasing rate as the density of states increases. A linear interpolation between reported values of the gap between the two valence bands at 298°K (Ref. 25) and 0°K (Ref. 23) gives a gap of 0.13 eV at 77°K. However, the value of E_F calculated from Eq. (23) for $p=4\times10^{18}$ cm^{-3} is only about 0.06 eV. Therefore the

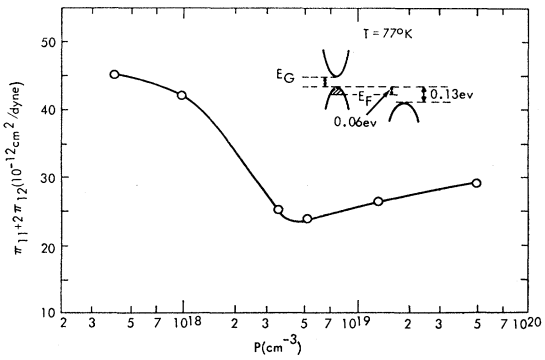

FIG. 15. Hole-concentration dependence of $\pi_{11}+2\pi_{12}$ at 77°K.

[58] R. E. Strakna and A. E. Clark (private communication).

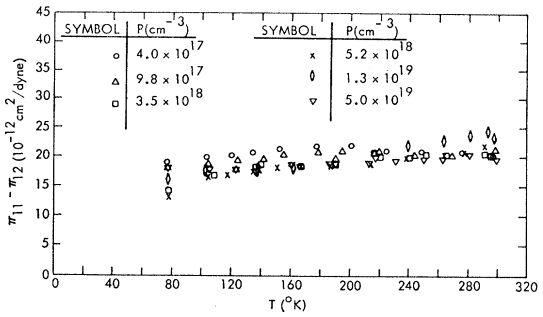

FIG. 16. Temperature dependence of $\pi_{11}-\pi_{12}$ for a range of hole concentrations.

increasing values of $\pi_{11}+2\pi_{12}$ cannot be attributed to the population of the second band and, at the present time, this behavior is not understood.

C. $\pi_{11}-\pi_{12}$

The coefficient $\pi_{11}-\pi_{12}$ is also a measure of the resistivity change produced by a shear stress. In this case however, the degeneracy of the ⟨111⟩ valleys is not removed and there is no carrier-transfer effect such as leads to the large values of π_{44}. The temperature dependence of this coefficient, as a function of carrier concentration, is shown in Fig. 16. These data have not been corrected for dimensional changes. This correction would increase these values by about 20% over the temperature range measured. The corresponding elastoconductivity

$$\frac{m_{11}-m_{12}}{2}=-(\pi_{11}-\pi_{12})\frac{C_{11}-C_{12}}{2} \tag{29}$$

is very nearly temperature-independent due to the 18% increase in $(C_{11}-C_{12})/2$ between 298 and 77°K. The average value of $(m_{11}-m_{12})/2$ is about 10. This value is 5 times larger than the elastoconductivity 2γ that was computed from the pressure dependence of the frequency of vibration of a lattice of harmonic oscillators. In addition, a change in the phonon spectrum is not expected for this strain because of crystal symmetry. Band calculations by Lin and Kleinman[48] and Conklin, Johnson, and Pratt[59] have shown that the valence band closest to the ⟨111⟩ extrema at L is a ⟨110⟩ band with extrema between Γ and K rather than at Γ as previously suspected. The coefficient $(m_{11}-m_{12})/2$ can be large for such a band because of the carrier-transfer effect.[40] Were this the reason for the large values of $(m_{11}-m_{12})/2$, one would expect a significant decrease in going to lower temperatures as observed in the coefficient $(m_{11}+2m_{12})/3$ when the second band is depopulated.

Pikus and Bir[41] have shown that for extrema at L, small contributions to $(m_{11}-m_{12})/2$ of the order of magnitude we observe occur if one or more nearby L extrema are degenerate. Due to the splitting of these extrema by the strain, one can see from the formulas for the effective mass given by Lin and Kleinman[48] for example, that the resulting energy-gap changes would lead to a change in effective mass. However, all experimental results and band calculations show that the principal bands at L are nondegenerate. For this case, energy shifts in the states at L are forbidden by crystal symmetry, and there should be no contribution to $(m_{11}-m_{12})/2$.

V. SUMMARY AND CONCLUSIONS

The temperature and hole concentration dependence of the shear coefficient π_{44} clearly show that the majority holes reside in a ⟨111⟩ multivalley band. The shear deformation potential Ξ_u of this band was found to be 8.5 eV. However, detailed calculations using existing theory and previously reported band parameters give much smaller values of π_{44} than observed experimentally. The theory was extended by means of a nonparabolic band model. The complete inadequacy of this model and of other considerations strongly suggests the need for radical changes in the band parameters used in the calculation. For example, recent neutron-diffraction measurements have revealed the presence of a low-lying optical branch and that in general the phonon spectrum of PbTe is quite complicated.

There are two mechanisms which contribute to the hydrostatic coefficient $\pi_{11}+2\pi_{12}$, the volume dependence of the transverse mass m_T and the presence of minority holes at high temperatures and concentrations. The deformation potential of the gap between the two valence bands was found to be about −1.0 eV.

The shear coefficient $\pi_{11}-\pi_{12}$ was surprisingly large, the corresponding elastoconductance being at least half that obtained from the effect of pure dilatation on the transverse mass of the ⟨111⟩ band. The temperature and concentration dependence show however that this is not due to the multivalley nature of the second valence band.

ACKNOWLEDGMENTS

I wish to express my gratitude to the Applied Physics Department of the Naval Ordnance Laboratory for their support of the thesis research. I am particularly indebted to Dr. Robert S. Allgaier and Dr. Bland Houston for their guidance during the course of this work. Several rewarding discussions were had with Professor Paul H. Meijer of Catholic University and Dr. Jack R. Dixon. The time and care taken by Elmer Gubner in preparation of the samples used is greatly appreciated. Finally, I wish to thank Dr. R. F. Greene and Dr. J. R. Cullen for their review of the manuscript.

[59] J. B. Conklin, Jr., L. E. Johnson, and G. W. Pratt, Jr., Phys. Rev. **137**, A1282 (1965).